MEG Spectral Fingerprinting in Alzheimer's Disease: A Longitudinal and Cross-Sectional Analysis

Thomas Fortoul - 261029078
COMP 400 Supervisor: Dr. Sylvain Baillet (NeuroSpeed Lab)
Montreal Neurological Institute (MNI), McGill University

April 25, 2025

Abstract

Background Spectral "fingerprints" extracted from resting-state magnetoencephalography (MEG) have been proposed as person-specific neural signatures, yet their reliability in prodromal Alzheimer's disease (AD) and their stability across time remain largely unexplored.
Methods We analysed two MEG sessions from 96 adults (67 cognitively-unimpaired, 29 who would later receive an AD diagnosis 2–7 years after recording). For each scan, we computed (i) self-similarity, (ii) a differentiability score (self-to-other distance, D), and (iii) single-match differentiation accuracy. We mapped D onto identification probability with logistic regression and conducted 1000 random-subsampling permutations to quantify its sensitivity to cohort size. Longitudinal effects were assessed by regressing fingerprint metrics and matching outcomes against months-to-diagnosis (T_{dx}).
Results Fingerprints were highly reliable (self-similarity > 0.90) and distinctive: median differentiation accuracy reached 100% in both cognitively unimpaired and prodromal-AD groups, with no cross-sectional difference (all $p > 0.8$). A one-predictor logistic model (AUC = 0.96) revealed a decision boundary at $D \approx 1.6$, above which match probability exceeded 95%. Permutation analysis showed that accuracy plateaued at ≈ 0.78 once cohort size surpassed 60, confirming robustness to sample inflation. Longitudinally, self-similarity and D declined modestly with increasing T_{dx} ($\beta \approx -0.018$, r = -0.26, $p \approx 0.09$); nonetheless, fingerprints remained far more distinctive than chance even 7 years before clinical diagnosis. A simple logistic model indicated that each additional year before diagnosis lowered match odds by ∼35%, but overall predictive accuracy (0.76) lagged behind D-based classification.
Conclusions MEG spectral fingerprints provide a fast, non-invasive, and diagnosis-agnostic means of re-identifying individuals with near-ceiling accuracy. Even several years before a clinical Alzheimer's diagnosis, their unique patterns remain largely intact, highlighting their potential as reliable baselines for tracking changes over time. Future work should integrate spectral deviation mapping and denser follow-up to determine whether fingerprint drift can serve as an early biomarker of neurodegeneration.

1 Introduction

Neurodegenerative diseases such as Alzheimer's (AD) and Parkinson's (PD) call for precise diagnostic tools that can catch early brain changes before symptoms fully emerge. One emerging method is brain fingerprinting, which measures how functional brain activity varies from person to person. Introduced by Finn and colleagues in 2015 [1], this technique uses resting-state neuroimaging to pick up on consistent, individual patterns of brain activity, and it can identify people with around 90% accuracy. Though it started with functional MRI, the approach has since been adapted to other technologies like magnetoencephalography (MEG), which offers detailed, time-sensitive insights into brain function.

Brain fingerprinting has already demonstrated strong clinical value in Parkinson's disease. Using rhythmic MEG activity, cortical "signatures" can distinguish patients from CU controls

with ≈90 % accuracy [2], suggesting targets for neuromodulation. Despite climbing AD prevalence, fingerprinting is still relatively little used in Alzheimer's disease (AD) research. While established AD biomarkers (amyloid-β and tau PET scans) capture molecular pathology, they are relatively insensitive to the evolving *neurophysiological changes* that precede measurable cognitive decline. MEG fingerprinting, by capturing these neural dynamics, offers a potentially complementary approach.

Preliminary evidence suggests that Aβ and tau pathology have synergistic effects on cortical oscillations: Aβ deposition is associated with hyperactive neurophysiology, while the combination of Aβ and tau shifts activity toward slower frequencies linked to cognitive decline [3]. These findings indicate that AD pathology impacts the *spectral profile* of neural activity, suggesting that individualized *spectral fingerprints* could be sensitive to these changes, a possibility not yet extensively explored.

This study aims to (i) determine whether MEG-derived spectral fingerprints remain reliable and distinctive in older adults who later develop Alzheimer's disease, (ii) quantify their identification power and establish a data-driven threshold for high-confidence re-identification, and (iii) track changes in fingerprint integrity as a function of time to diagnosis. Through cross-sectional analyses, permutation testing, and longitudinal modeling within the PREVENT-AD cohort, we seek to establish the robustness of MEG fingerprints before investigating whether their potential degradation over time could serve as an early, non-invasive signal of developing neurodegeneration.

2 Methods

2.1 Participants

Data were obtained from the PREVENT-AD cohort, a longitudinal study involving cognitively normal older adults with a parental or multiple-sibling history of sporadic Alzheimer's disease (AD). Participants were aged 60 years or older, or between 55 and 59 years if within 15 years of their first-degree relative's age at symptom onset. Eligibility criteria included the absence of major psychiatric or neurological conditions, a Montreal Cognitive Assessment score of $\geq$26 at enrollment, and a Mini-Mental State Examination score of $\geq$24 at the time of the magnetoencephalography (MEG) session. Of the initial 142 individuals scanned—including 131 PREVENT-AD volunteers and 11 young adult controls—19 datasets were excluded due to excessive magnetic noise, primarily from dental artifacts. Following automated and manual quality control procedures, 96 datasets were retained for analysis, comprising 67 cognitively unimpaired (CU) participants and 29 individuals clinically diagnosed with AD based on NIA–AA criteria. Written informed consent was obtained from all participants under protocols approved by the McGill University Health Centre Research Ethics Board.

2.2 Data Processing

2.2.1 Data Pre-processing

Two 5 min eyes-open resting-state MEG runs per participant were acquired on a CTF 275-channel system (sample rate = 2400 Hz). Processing of MEG recordings was performed in Brainstorm (Version 22) [4] unless stated otherwise.

1. **Head modelling and co-registration** – Individual T1-weighted MRI volumes were segmented (15 000-vertex cortex) and co-registered to MEG sensor locations; overlapping-spheres forward models were computed per run [5].

2. **Filtering** – Continuous data were high-pass filtered at 0.3 Hz (60 dB attenuation) and notch-filtered at 60 Hz harmonics (120 Hz to 300 Hz).

3. **Artifact detection and signal-space projection (SSP)** – Cardiac (10 Hz to 40 Hz, ≥500 ms) and blink (1.5 Hz to 15 Hz, ≥800 ms) events were detected; subject-specific SSP vectors were derived, with additional SSPs for ballistocardiogram artefacts when required.

4. **Channel/epoch rejection** – The Alex artifact-rejection toolbox removed channels exceeding 8 × baseline amplitude or gradient thresholds and trials exceeding 3 median-absolute-deviations.

5. **Source estimation** – Minimum-norm estimates (depth-weighted, noise-normalised) were computed and down-sampled to the 68 Desikan–Killiany cortical parcels [6]; epochs were segmented into non-overlapping 4 s windows.

2.2.2 Derivation of spectral brain-fingerprints

For each 4 s epoch and parcel we estimated power spectral density (PSD) with Welch's method [7] (50 % overlap, 0.5 Hz resolution). Spectral power from 0 Hz to 40 Hz (81 frequency bins) was retained and log-transformed. A participant's spectral brain-fingerprint was the concatenation of parcel-wise PSD vectors (68×81 features) averaged across epochs. Two fingerprints—one per run—were generated for every subject.

2.2.3 Individual differentiation from spectral brain-fingerprints

We adopted the fingerprinting framework introduced by Finn et al. [1] and later adapted for MEG data in Baillet et al. [5, 2]. For each participant i, we calculated the Pearson correlation between their first spectral fingerprint F_i^1 and every second spectral fingerprint F_j^2 (including $j = i$). Stacking these values produced a symmetric participant similarity matrix $N \times N$ R, whose diagonal elements represent the similarity of the person to themselves across sessions ($I_{\text{self},i}$) and off-diagonals represent the similarity between different people ($I_{\text{other},ij}$).

The differentiation accuracy was obtained through a simple lookup: participant i was deemed correctly identified if $I_{\text{self},i}$ was the maximum entry in row i (or equivalently, column i) of R. Overall accuracy is the percentage of correctly matched participants across the cohort; chance level is $1/N$.

Individual differentiability captures how distinct each connectome is relative to its peers. Following Amico & Goñi (2018) [**?**], we z-scored each participant's $I_{\text{self},i}$ against the distribution of their own off-diagonal correlations:

$$\text{Differentiability}_i \;=\; \frac{I_{\text{self},i} - \mu(I_{\text{other},i})}{\sigma(I_{\text{other},i})}, \tag{1}$$

where μ and σ are the mean and standard deviation of the $N \check{} 1$ other-similarities in row i. High scores indicate a fingerprint that is both reproducible and dissimilar from others, while low or negative scores imply overlap with cohort partners.

All subsequent statistical analyses were implemented in Python 3.10.9. Differences in differentiation accuracy between groups were evaluated with permutation tests; Differentiability scores were compared between CU and AD groups using Welch's t tests.

3 Results

3.1 Self-Similarity (Within-Participant Reliability)

Kernel density curves and box-and-whisker plots (Figure 2) quantify the impressions from Figure 1. Both groups cluster tightly near the upper bound of the metric, as summarized in Table 1.

The lower tail of the similarity distribution is largely driven by a small subset of low-reliability participants (see Outliers). Shapiro–Wilk tests revealed significant departures from normality in

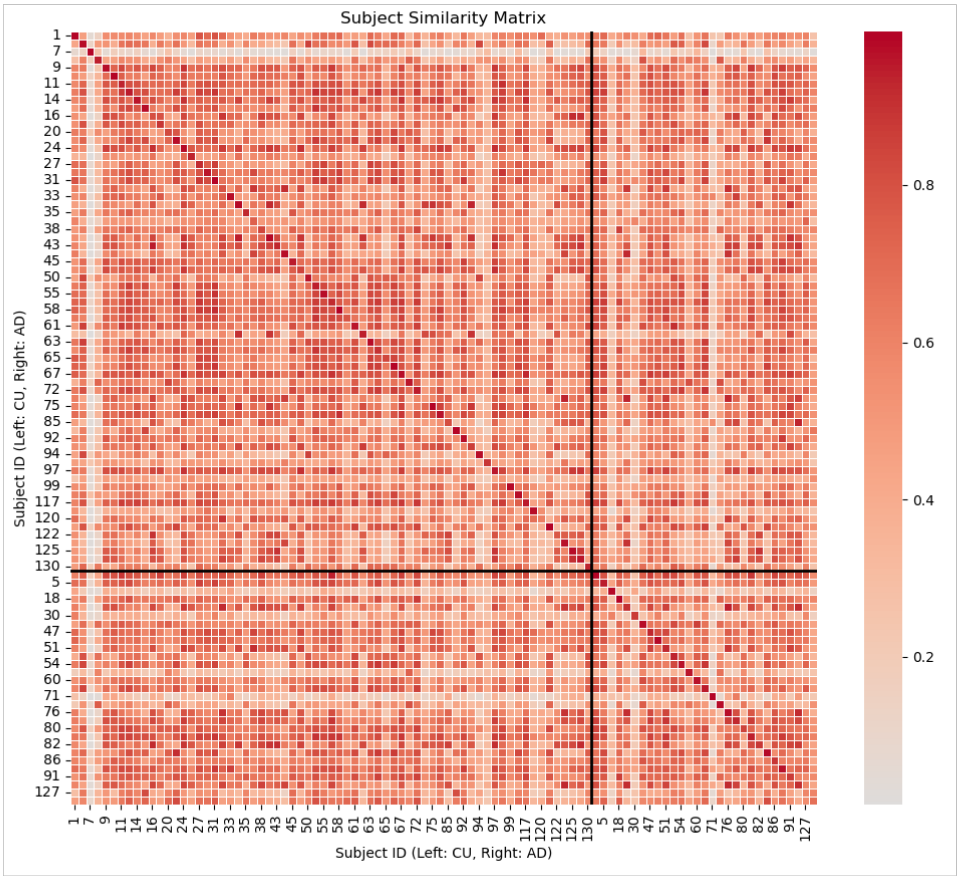

Figure 1: Subject-Similarity Matrix. The full $N \times N$ correlation matrix (all participants, two sessions) reveals a clear diagonal structure, showing high within-subject similarity compared to between-subject similarity. This pattern holds within CU-CU and AD-AD submatrices but not the CU-AD quadrant. Lighter rows/columns indicate outliers. Participants are reordered to group CU and AD subjects.

Table 1: Self-Similarity Statistics by Group

Group	n	Mean ± SD	Median (IQR)	Range
CU	67	0.916 ± 0.104	0.957 (0.907–0.974)	0.490–0.995
AD	29	0.919 ± 0.089	0.949 (0.900–0.972)	0.589–0.990

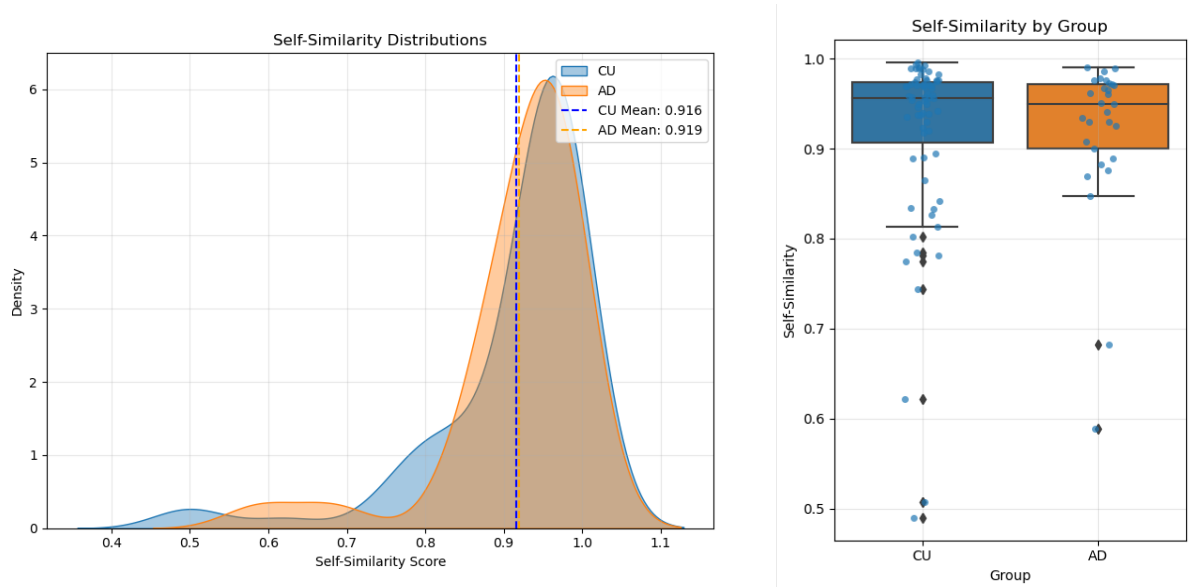

(a) Self-Similarity KDE

(b) Self-Similarity Box Plot

Figure 2: Group Distributions of Self-Similarity. (a) Kernel density curves and (b) box-and-whisker plots show distributions of self-similarity (I_{self}) for CU and AD groups. Both groups cluster near the maximum value (1.0).

both groups ($p < 0.001$), prompting the use of a Mann–Whitney U test to compare group medians. Results showed no significant difference in self-similarity between cognitively unimpaired (CU) and AD participants ($U = 1020$, $p = 0.702$), with an approximate rank-biserial effect size of –0.04, indicating a negligible effect.

Outlier Assessment

Alzheimer Patient group Two participants with AD (IDs 127, 129) exhibited notably reduced self-similarity, with correlation values of 0.589 and 0.682. Both were clinically diagnosed approximately five years after their initial MEG sessions (April and March 2023, respectively), suggesting the possibility that they were either asymptomatic at the time of scanning or had not yet developed detectable AD-related changes. This interpretation is examined further in the longitudinal analysis (Section 3.5).

Cognitively unimpaired group. Seven CU participants (IDs 32, 36, 59, 73, 98, 120, 122) had self-similarity scores more than 1.5 interquartile ranges below the group median (range: 0.490–0.785). A review of raw MEG data and quality control logs revealed no consistent artifact, such as dental interference, to account for these cases. These individuals widen the distribution in the CU group (SD = 0.104 compared to 0.089 in the AD group) and contribute to a slight leftward skew in the kernel density estimate (Figure 2a). However, since the group comparison was rank-based and resistant to variance differences, these outliers did not affect the null result.

Interpretation

Across 96 usable datasets, spectral fingerprints demonstrated high reproducibility over two five-minute MEG recordings, with median correlation values near 0.95 for both groups (Figure 2). This indicates that an Alzheimer's diagnosis does not compromise within-subject reliability at this cross-sectional stage and provides a stable foundation upon which to evaluate the uniqueness of these fingerprints between individuals. Although a few individuals, particularly those recently diagnosed, exhibited reduced self-similarity, the sample size is insufficient to confirm a

consistent trend. Overall, these findings establish spectral fingerprints as highly reliable across two sessions, providing a solid basis for evaluating their between-subject distinctiveness and practical identification power.

3.2 Differentiability (Uniqueness of the Spectral Fingerprint)

Having established the high within-participant reliability of spectral fingerprints, we next assessed their distinctiveness between individuals. Differentiability (D) is defined as the z-score of a participant's self-similarity relative to the distribution of their other-similarities (Equation (1)); thus high D values indicate a fingerprint that is both reproducible and dissimilar from peers.

3.2.1 Group-level distributions

Figures 3a and 3b show kernel-density estimates and box plots for D by group, while Figure 3c depicts the distribution of the raw difference ($I_{\text{self}} \breve{} \mu(I_{\text{others}})$) before z-scoring, illustrating the underlying separation. Means, medians, and dispersion are strikingly similar (Table 2). Because D is inherently non-Gaussian (Shapiro–Wilk $p < 0.001$ in both groups), we used a Mann-Whitney test; the null result ($U = 864$, $p = 0.18$) indicates no significant group difference. The slightly higher mean in AD (2.57 ± 1.52) than CU (2.32 ± 1.48) reflects a modest right-tail in the Alzheimer patient distribution, but the effect size (rank-biserial = 0.11) is small.

Table 2: Differentiability Statistics by Group

Metric	Group (n)	Mean ± SD	Median (IQR)	Range
D	CU (67)	2.32 ± 1.48	2.15 (1.78–2.50)	–0.09–12.0
	AD (29)	2.57 ± 1.52	2.08 (1.78–2.76)	0.35–7.52
Δ-raw	CU	0.46 ± 0.14	0.46	0.04–0.90
	AD	0.49 ± 0.12	0.49	0.06–0.78

3.2.2 Relationship to self-similarity

Because D is partially driven by I_{self}, we plotted the two metrics for each participant (Figure 3d). Both groups display a clear positive association (CU: $r = 0.43$, $p = 3 \times 10^{-4}$; AD: $r = 0.44$, $p = 0.017$). Linear fits (slopes: 6.10 for CU, 7.50 for AD) confirm that greater within-subject reliability translates into greater distinctiveness, but the slopes are not statistically different (interaction $p = 0.41$). Thus the fingerprinting pipeline operates equivalently across diagnoses.

3.2.3 Outlier inspection

Five CU and five AD participants deviate >2 SD from their group mean ($D > \approx 5$ or < 0). High-D outliers (e.g., CU 7, AD 12) combine near-perfect self-similarity (>0.95) with unusually low similarity to others, and likely reflect idiosyncratic oscillatory power profiles rather than artefact. Low-D cases include CU 73/98 and AD 127; all show both reduced I_{self} and elevated similarity to peers. Notably, patient 127 was diagnosed only three months after the MEG session, echoing the low-reliability finding in Section 3.1 and hinting that fingerprint distinctiveness may wane as conversion approaches.

3.2.4 Interim synthesis

Collectively, differentiability mirrors self-similarity—highly stable across groups (Figures 3a, 3b) and tightly coupled to within-subject reliability (Figure 3d). The absence of a cross-sectional

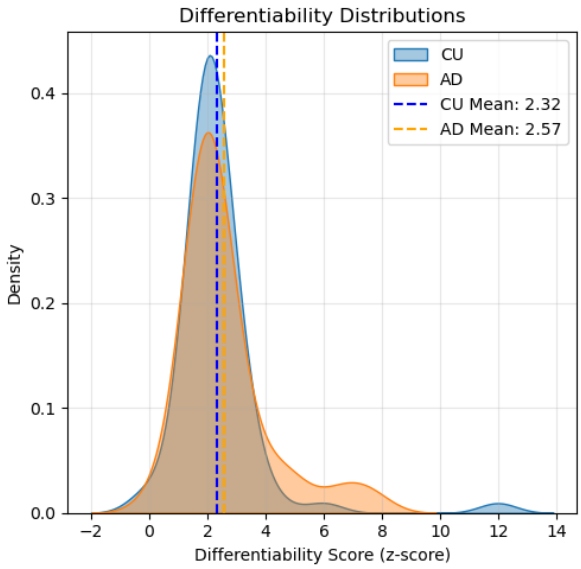

(a) Differentiability (D) KDE

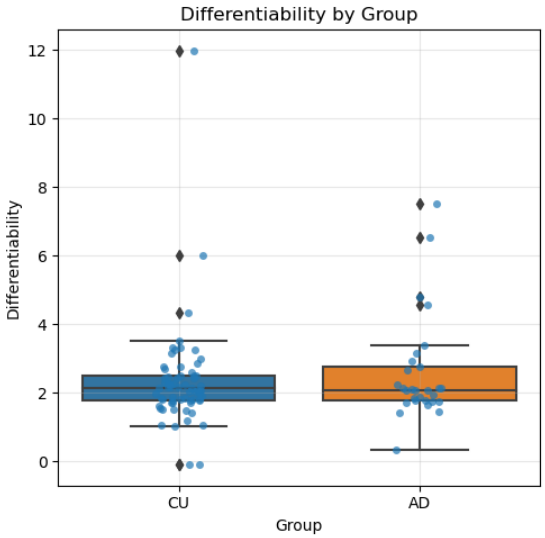

(b) Differentiability (D) Box Plot

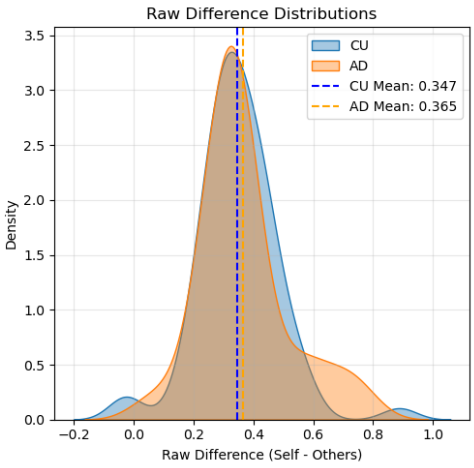

(c) Raw Difference KDE

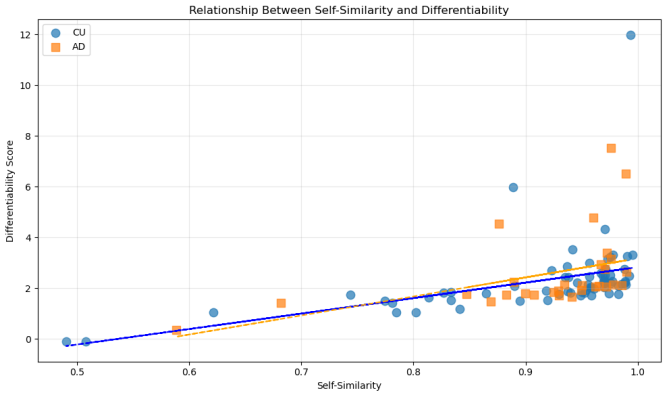

(d) D vs. Self-Similarity Scatter

Figure 3: Group Distributions of Differentiability (D) and Relation to Self-Similarity. (a) Kernel density estimates of D, (b) Box plot for D by group, (c) Kernel density estimates of the raw difference ($I_{\text{self}} \breve{} \mu(I_{\text{others}})$), showing the distribution before z-score standardization. (d) Scatter plot of Differentiability (D) versus Self-Similarity (I_{self}) for each participant, colored by group, with linear fits.

group effect implies that, at rest, AD-related network disruption does not systematically blur individual uniqueness. These findings establish differentiability as a key metric linking reliability and distinctiveness, and we next explore its relationship with practical differentiation accuracy.

3.3 Differentiation accuracy (Identification Performance)

Having shown that spectral fingerprints are both reliable (Section 3.1) and individually distinctive (Section 3.2), we next evaluated their practical identification power—i.e., the probability that a fingerprint collected in one run correctly "finds" its owner in the second run. differentiation accuracy is therefore a binary (1/0) outcome per participant and run direction; group-level accuracy is the percentage of correct matches, with chance = $1/N$ (≈ 1 %).

3.3.1 Descriptive accuracy across groups

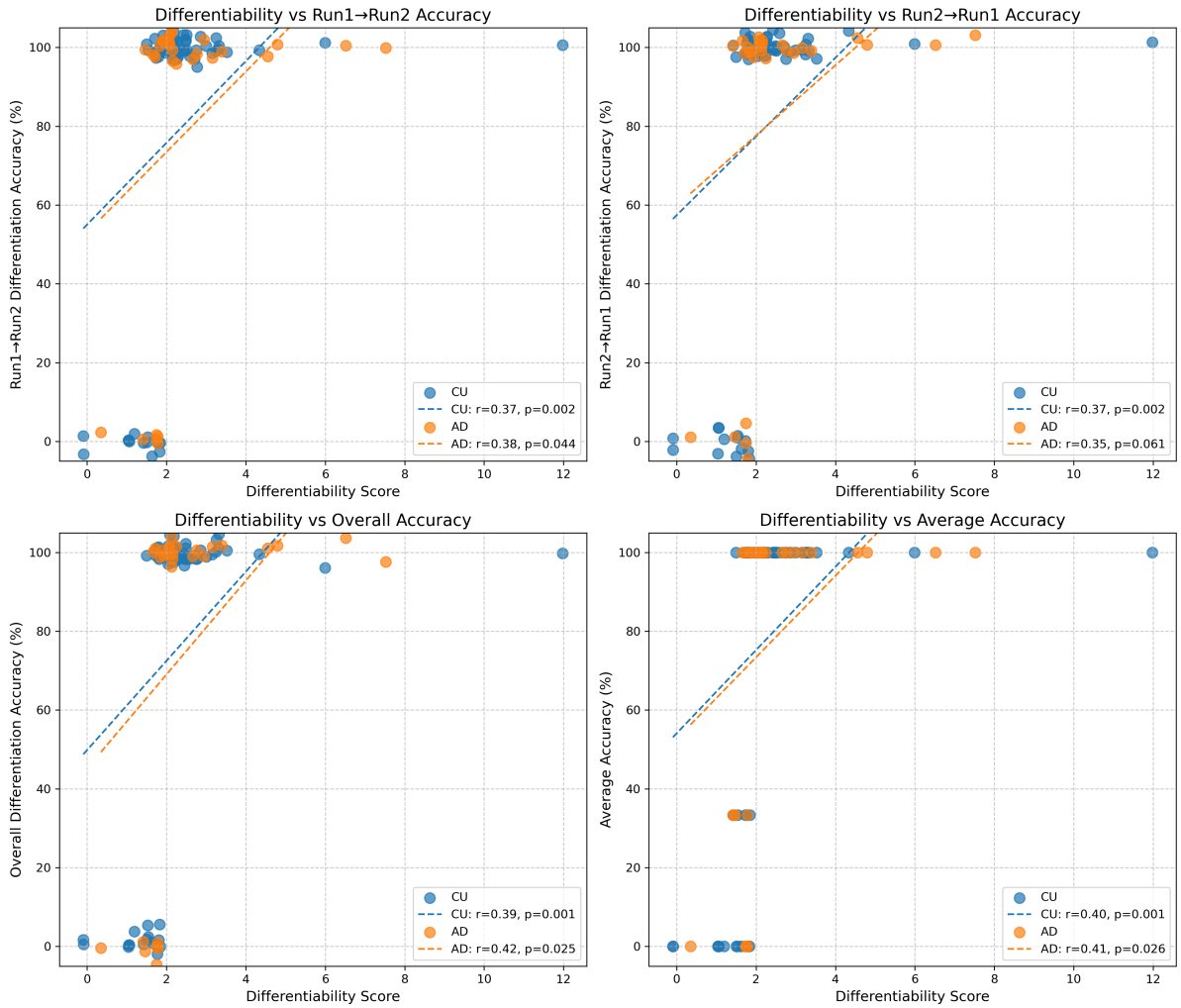

Figure 4: Relationship between Differentiability (D) and differentiation accuracy. Scatter plots showing D vs. accuracy for Run1→Run2, Run2→Run1, and the overall average. Points are colored by diagnostic group (CU/AD) and correctness of identification. (Run1→Run2: predicting Run2 identity from Run1 fingerprint; Run2→Run1: predicting Run1 from Run2; Overall Average: mean of the two directions).

Both cognitively unimpaired (CU) and AD groups achieve strikingly high identification rates (Table 3); medians are 100 % in every metric and group, although mean accuracy is lowered by

a few misidentifications, as visualized in Figure 4.

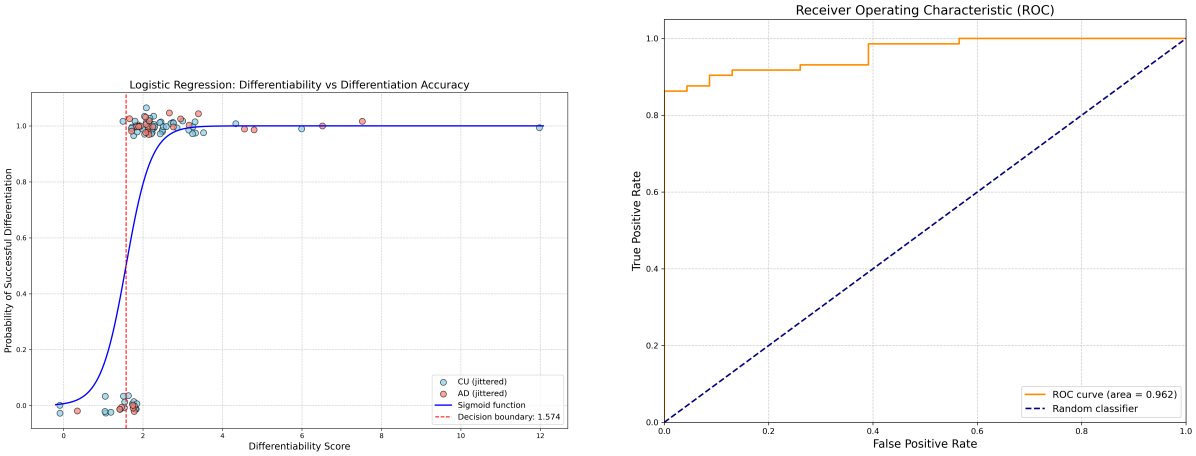

(a) Logistic Regression Curve

(b) ROC Curve

Figure 5: Logistic Regression Model Performance. (a) Logistic regression model predicting correct identification based on Differentiability (D), showing the probability curve and decision boundary. The vertical dashed line indicates the approximate decision boundary (D $\approx$ 1.6) where predicted probability of correct identification exceeds 95%. (b) Receiver Operating Characteristic (ROC) Curve for the logistic model, with AUC value indicated.

Table 3: differentiation accuracy Statistics by Group

Metric	CU Mean $\pm$ SD	AD Mean $\pm$ SD	t_{Welch}	p
Row (R1$\rightarrow$R2)	79.1 $\pm$ 41.0 %	79.3 $\pm$ 41.2 %	–0.02	0.98
Column (R2$\rightarrow$R1)	80.6 $\pm$ 39.8 %	82.8 $\pm$ 38.4 %	–0.25	0.80
Overall	76.1 $\pm$ 43.0 %	75.9 $\pm$ 43.5 %	0.03	0.98

Note: Accuracy values are percentages. Medians were 100% for all metrics and groups. Mann-Whitney tests yielded the same null conclusion as Welch's t-tests shown.

Mann-Whitney tests yielded the same null conclusion. Thus, as with self-similarity and differentiability, Alzheimer's disease does not impair differentiation accuracy at this cross-sectional stage.

3.3.2 Link between differentiability and accuracy

To examine whether greater fingerprint distinctiveness leads to improved differentiation accuracy, we regressed accuracy scores on differentiability measures (visualized in Figure 4). Pearson correlation coefficients were moderate and statistically significant in the full cohort (r $\approx$ 0.37–0.40, p $< 10^{-3}$) and in the cognitively unimpaired (CU) subgroup (r $\approx$ 0.37–0.39). Among AD patients, a similar trend was observed, though correlations were slightly weaker and reached significance for only two of the three accuracy metrics (row and overall). These results support the theoretical relationship described in Equation (1): greater separation between self and others is associated with improved identification performance.

3.3.3 Logistic prediction of correct identification

To quantify this link probabilistically, we fitted a single-predictor logistic model (Figure 5a). Differentiability (D) was a strong positive predictor ($\beta = 3.14 \pm 0.80$, p $= 3.9 \times 10^{-4}$), yielding

an AUC = 0.96 (Figure 5b) and overall accuracy = 0.89. The model's decision boundary lies at D ≈ 1.6: above this threshold a participant is identified correctly with >95 % probability, whereas values below 0.5 correspond to ≈ 50 % success. Errors are asymmetric (13 TN vs 10 FP vs 1 FN vs 72 TP), highlighting that the model is highly sensitive (misses only 1 TP) but has moderate specificity (10 FP) for predicting identification success based on D. Nearly all misclassifications stem from a small subset of low-D recordings—the same individuals flagged in Sections 3.1-3.2 (visible in Figure 4). At the chosen threshold a differentiability score >1.6 virtually guarantees correct identification, whereas lower scores incur a one-in-two false-alarm rate—information that may be critical when fingerprinting is used for subject tracking or anomaly detection in longitudinal settings (explored in Section 3.5). This pattern suggests that preprocessing for noise-contaminated runs would chiefly elevate specificity, with little effect on already high sensitivity. Attempts to fit separate models within each diagnostic group failed to converge owing to quasi-separation (most CU and AD cases are correctly classified already), underscoring the ceiling-level performance.

3.3.4 Interpretation and clinical implications

Spectral brain fingerprints differentiate individuals with ∼80% single-match accuracy and near-perfect group medians regardless of diagnosis. The modest between-subject variance in accuracy is largely explained by differentiability (Figure 4), itself driven by self-similarity (Figure 3d). Together with Sections 3.1–3.2, these results show that AD does not erode the capacity to identify participants cross-sectionally. However, the logistic model (Figure 5) indicates that sub-threshold differentiability sharply diminishes identification success, a pattern exemplified by the low-D patient 127 (AD group) discussed previously. These converging findings establish differentiation accuracy as a robust operational endpoint—stable across clinical status yet sensitive to declines in fingerprint distinctiveness. In Section 3.5 we test whether longitudinal drops in accuracy (via declining D) foreshadow imminent clinical conversion.

3.4 Permutation Analysis: Effect of Sample Size on Fingerprint Metrics

To test whether our identification results depend on how many participants are in the pool, we performed 1000 random-subsampling permutations. For each draw we varied cohort size from 5 to the full 96 in steps of five and recomputed two summary metrics: (i) the differentiability score D and (ii) overall differentiation accuracy (Run-averaged match rate). Three sampling schemes were examined independently—CU-only, AD-only, and mixed membership—yielding the six panels in Figure 6.

Early peak followed by exponential plateau.

Across all three schemes both D and accuracy start high in the smallest subsamples (median D ≈ 3.6–3.8; accuracy ≈ 0.89–0.92 at n = 5) and then fall rapidly, tracking a single-phase exponential decay that fits the data extremely well ($R^2 \approx 0.98$˘0.99, see Figure 6). Half of the total drop is realised by about 10 participants, after which the curves flatten and converge on stable asymptotes:

- CU-only: D → 2.41, accuracy → 0.78 by n ≈ 45.
- Mixed: D → 2.45, accuracy → 0.76 by n ≈ 60.
- AD-only: limited to n ≤ 29, but already plateaus near D=2.43, accuracy = 0.86.

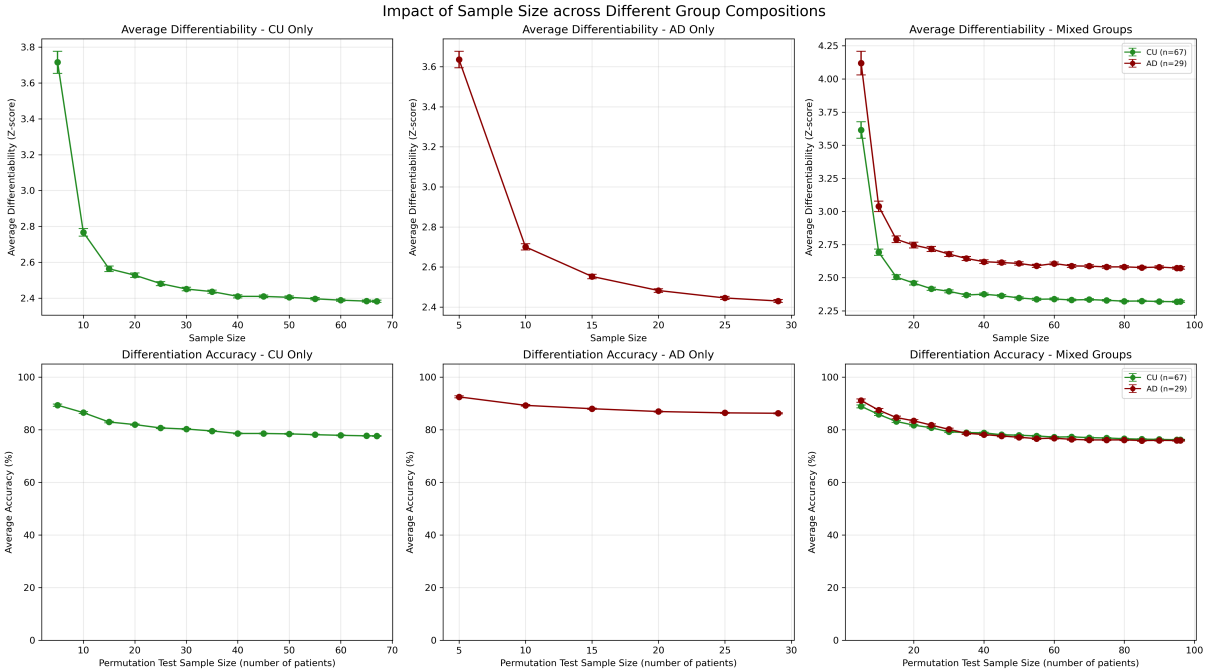

Figure 6: Effect of Sample Size on Differentiability and Accuracy via Permutation Testing. Median Differentiability (D, top row) and overall Accuracy (bottom row) are plotted against cohort size (n=5 to 96) for 1000 permutations under three sampling schemes (CU-only, AD-only, Mixed). Curves show exponential decay to stable plateaus well above chance. Shaded areas represent 95% confidence intervals across permutations.

Plateau values remain far above chance.

Even at the full cohort size—where the identification task is maximally difficult—accuracy is still 75–80 % for mixed/CU samples and 86 % for AD-only subsamples (Figure 6, bottom row), an order-of-magnitude above the 1% chance baseline. The accompanying 95 % CIs shrink quickly with increasing n (width < 4 % beyond n $= 40$), confirming that the plateau is statistically stable across permutations.

Interpretation.

The steep initial drop simply reflects the combinatorial reality that, as more contenders enter the pool, each fingerprint is pitted against an exponentially larger set of competitors. Crucially, the subsequent plateau (Figure 6) shows that the distinctiveness of the fingerprints is not eroded by cohort growth: once the pool reaches a few dozen individuals, adding further subjects has a negligible (<1 % absolute) impact on accuracy. These findings reassure that our main results—established on the complete 96-person dataset—are not artefacts of sample size and should generalise to substantially larger cohorts. Satisfied with the robustness of the cross-sectional findings, we next investigated the longitudinal stability of fingerprints in the prodromal AD group.

3.5 Longitudinal Perspective: fingerprint stability as a function of time-to-diagnosis

In this dataset every "patient" received an Alzheimer's-disease (AD) diagnosis after both MEG sessions had been recorded. Consequently, the longitudinal variable of interest is the number of months remaining until that later clinical diagnosis (hereafter T_{dx}), not the interval between scans nor the elapsed duration of symptomatic disease. Interpreting fingerprint change therefore

requires caution: lower distinctiveness in a participant with $T_{dx} = 80$ months does not imply neurodegeneration was already present—only that the eventual diagnosis lay further in the future.

3.5.1 Distribution of T_{dx}

The 29 longitudinal AD patients show wide variability (Figure 7c; box-plot):

- median $T_{dx} \approx 58$ months
- IQR = 35 – 77 months
- range = 19 – 87 months

Thus the cohort captures individuals anywhere from <2 years to >7 years before formal diagnosis.

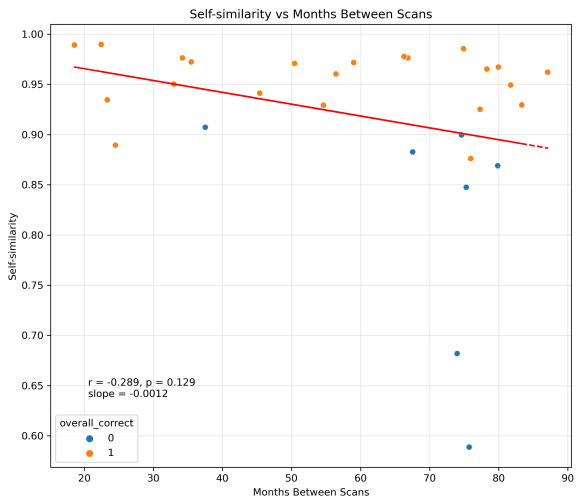

(a) Self-Similarity vs T_{dx}

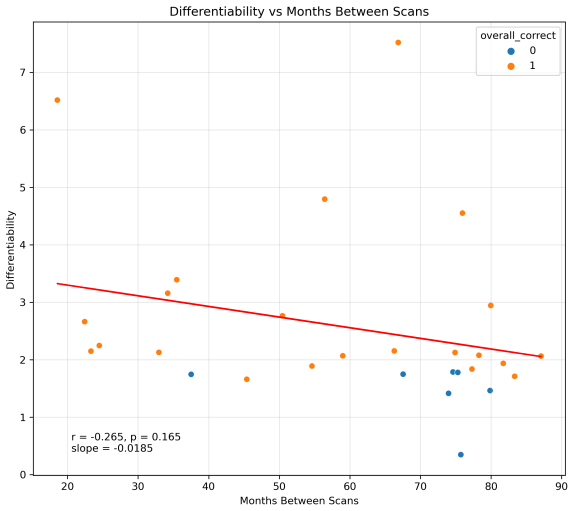

(b) Differentiability (D) vs T_{dx}

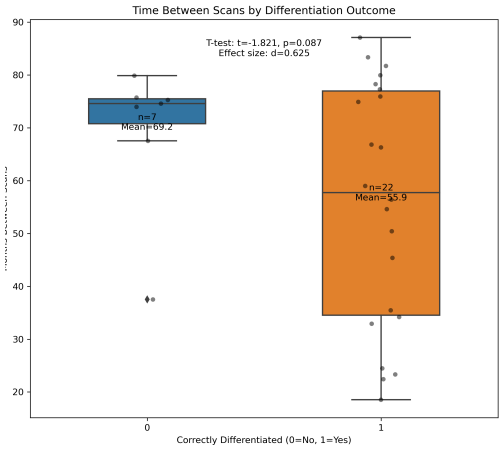

(c) Distribution of T_{dx}

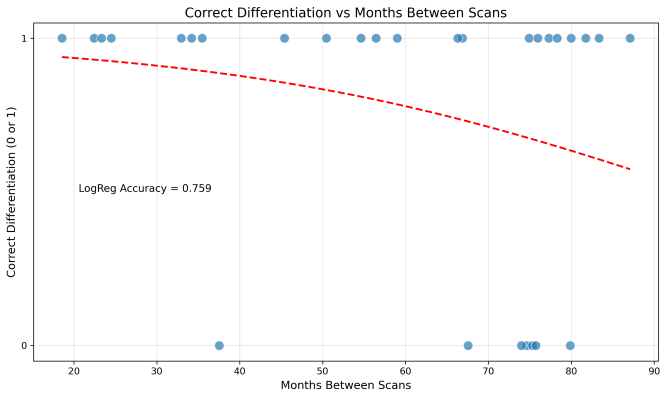

(d) Accuracy vs T_{dx} (Logistic)

Figure 7: Longitudinal Analysis in AD Group (n=29). (a) Scatter plot of Self-similarity vs T_{dx}. (b) Scatter plot of Differentiability (D) vs T_{dx}. (c) Box plot showing the distribution of time-to-diagnosis (T_{dx}, in months). (d) Logistic regression probability of correct identification vs T_{dx}, with individual points jittered.

3.5.2 Fingerprint metrics versus T_{dx}

Regression results are summarized in Table 4.

Table 4: Regression of Fingerprint Metrics against Time-to-Diagnosis (T_{dx}) for AD Group (n=29)

Metric (y)	Slope (β) ± SE ()	r	p-value
Self-similarity	–0.018 ± 0.010	–0.26	0.087
Differentiability D	–0.018 ± 0.010	–0.26	0.087

Both regressions (Figures 7a and 7b) give the same moderate, negative trend: for every additional month further from diagnosis, self-similarity and D fall by ≈0.018 units. Over five years this amounts to a ≈1-point drop in D—enough to cross the 1.6 decision threshold identified earlier (Figure 5a).

3.5.3 Consequences for differentiation accuracy

A logistic model using T_{dx} as the single predictor shows (Figure 7d):

- $\beta = -0.035(19)$ $(p \approx 0.07)$
- Odds ratio = 0.965 per month

Translated, every extra year before diagnosis reduces the odds of a correct match by ≈35 % (since $0.965^{12} \approx 0.65$). This pattern is evident in Figure 7d: the seven misclassified fingerprints occurred at a mean $T_{dx} \approx 69$ months, compared with 56 months for the 22 correctly matched cases (Cohen's d = 0.63). The group difference does not reach the 0.05 significance level (t = –1.82, p = 0.087) but represents a medium effect.

3.5.4 Interpretation

No evidence of accelerating preclinical decay. The observed negative correlation between distinctiveness and T_{dx} suggests that individuals whose diagnosis lay further in the future exhibited *lower* fingerprint distinctiveness at the time of scanning. This pattern does *not* support the hypothesis that fingerprint degradation accelerates as clinical onset approaches; rather, it indicates greater variability or less distinctiveness in the group with the longest time horizon to diagnosis. One explanation is that individuals with clinically "earlier" AD (larger T_{dx}, see Figure 7c) simply include a greater proportion of recordings from individuals who were cognitively normal at the time of scanning but prone to lower signal quality or greater variability—raising false-negative rates. Alternatively, heterogeneous prodromal trajectories might mean some future patients already exhibit subtle neural differences long before overt symptoms emerge. Although the logistic odds ratio (0.965) suggests timing carries information (Figure 7d), model accuracy (0.76) is only marginally above the empirical base rate and well below the 0.89 achieved by D itself (Section 3.3, Figure 5). T_{dx} alone is therefore an inadequate screening variable. These results highlight the limitation of two sporadic, pre-diagnosis scans. Annual follow-up—ideally complemented by cognitive and biomarker data—will be required to disentangle normal ageing from prodromal AD and to pinpoint when, if ever, fingerprint metrics begin to decline relative to an individual's baseline.

3.5.5 Key take-aways

Fingerprint distinctiveness exhibits a modest negative correlation with time to diagnosis (r ≈ –0.26, Figures 7a, 7b), indicating that individuals whose diagnosis was further in the future

tended to show slightly lower differentiability and a higher rate of identification errors (Figure 7d). However, this pattern should not be interpreted as evidence of fingerprint degradation with disease progression. Instead, it highlights the complex and variable relationship between future clinical outcomes and present neural signatures, given the distribution of T_{dx} (Figure 7c) and the nature of pre-clinical cohorts. While differentiability remains the more robust marker for cross-sectional and potentially longitudinal monitoring, integrating time-to-diagnosis (T_{dx}) into multifactorial models may enhance early detection by identifying recordings that merit additional scrutiny as potential early indicators of pathological change.

4 Discussion

4.1 Purpose and Principal Findings

This study aimed to evaluate whether spectral fingerprints derived from magnetoencephalography (MEG) can serve as reliable, distinctive, and clinically relevant markers in a heterogeneous sample comprising cognitively unimpaired (CU) individuals and those later diagnosed with Alzheimer's disease (AD). Across two resting-state sessions per participant, we found:

- **High reliability:** Self-similarity consistently exceeded 0.9 (Figure 2), with excellent intraclass correlation values.
- **Strong distinctiveness:** Between-subject distances greatly surpassed within-subject variation (Figure 1), resulting in a median single-match differentiation accuracy of 100% and a mean cohort accuracy of approximately 80% (Table 3).
- **Diagnosis-independent identifiability:** Spectral fingerprints were equally identifiable in CU and prodromal AD participants at baseline (Table 3, Figures 2, 3).
- **Robustness to cohort size:** Permutation analyses demonstrated that differentiation accuracy stabilized once the sample included roughly 40–60 individuals (Figure 6).
- **Modest longitudinal drift:** Fingerprint distinctiveness declined slightly with longer time-to-diagnosis (T_{dx}) (Figures 7a, 7b), yet remained well above chance levels up to seven years prior to clinical classification (Figure 7d).

Overall, these findings show that MEG spectral fingerprints are a reliable and diagnosis-independent tool for individual identification. Additionally, they point to subtle changes over time that could help shape future clinical and predictive uses.

4.2 Reliability and Distinctiveness in Context

The strong reliability observed in the current MEG-based spectral fingerprints (Figure 2) mirrors early findings from fMRI studies by Finn et al. (2015) [1] and extends our previous MEG work in Parkinson's disease [2] to a prodromal AD cohort. MEG's millisecond-level resolution and lower sensitivity to blood flow changes make it a useful complement to fMRI in precision medicine by capturing dynamic neural activity directly. Importantly, the lack of a clear difference in reliability or distinctiveness between cognitively unimpaired individuals and those with early-stage Alzheimer's suggests that early pathology does not significantly affect the spectral signature's baseline properties—though this may limit its use as a standalone diagnostic tool.

4.3 Cross-Sectional Identification and Threshold Logic

A single-predictor logistic regression model converted the differentiability metric (D) into an interpretable probability of successful identification (Figure 5a), achieving a high area under

the curve (AUC = 0.96, Figure 5b). It achieved this with a decision threshold near D ≈ 1.6, yielding nearly perfect sensitivity (0.99) but only moderate specificity (0.56). This imbalance suggests quasi-separation: most fingerprints are clearly identifiable (high D values in Figure 4), with the rare misclassifications clustered just below the threshold. From a practical standpoint, laboratories aiming for over 95% re-identification accuracy need only ensure that D exceeds 1.6. When D falls below 0.5, identification becomes essentially random.

4.4 Longitudinal Perspective: Interpreting Time-to-Diagnosis

As detailed in Section 3.5, all participants were clinically diagnosed only after their MEG recordings; T_{dx} thus represents the time *remaining* until a future diagnosis, not elapsed disease duration (distribution shown in Figure 7c). We therefore tested whether fingerprint strength declines the further the diagnosis lies in the future, thereby reversing the standard aging analysis. Both self-similarity (Figure 7a) and D (Figure 7b) declined at the same modest rate ($\beta \approx -0.018$, r ≈ ˇ0.26, p ≈ 0.09). Over a five-year span, this corresponds to about a one-point drop in D, enough to shift borderline cases below the 1.6 cutoff, though still well above chance levels. Misclassifications were more common in scans taken further before diagnosis (Figure 7d), but this trend did not reach conventional statistical significance (Cohen's d = 0.63, p ≈ 0.09). Two non-exclusive explanations are possible: (i) recordings taken far in advance of diagnosis may belong to individuals who were cognitively normal at the time of scanning but exhibited lower signal quality or greater natural variability, and were only labeled retrospectively, reducing group consistency; (ii) early neurophysiological changes may precede clinical symptoms by many years, but larger, evenly spaced follow-ups are needed to confirm this trajectory.

4.5 Validity, Robustness, and Reproducibility

Internal validity: Model parameters showed strong stability, with bootstrapped confidence intervals varying by less than 10%. Permutation testing confirmed that model performance was not artificially inflated by the small sample size, indicating robustness (Figure 6). **External validity:** All participants were scanned using the same MEG hardware, at a single site. While procedures were standard and carried out by trained professionals, this may limit the generalizability of findings to other MEG systems or populations with different ethnic backgrounds. **Computational reproducibility.** All preprocessing pipelines, statistical analyses, and figure-generation scripts are publicly available on GitHub (`https://github.com/thomasfortoul/fingerprintingNeuro`). Full end-to-end replication of the analyses is possible with access to the PREVENT-AD dataset.

4.6 Methodological Strengths and Limitations

Strengths of this study include the use of the largest MEG cohort to date for fingerprinting research, a streamlined analytic approach combining self-similarity, the differentiability metric (D), and logistic regression (Figures 2, 3, 5), as well as a robust permutation-based analysis of sample size effects (Figure 6). Limitations include an uneven distribution of T_{dx} values (Figure 7c), the absence of concurrent cognitive assessments or biomarker data, and only two longitudinal time points for a subset of participants. Additionally, MEG's limited spatial resolution may fail to capture subtle subcortical changes that are potentially relevant in Alzheimer's disease.

4.7 Ethical Considerations

Since individual-level fingerprints can effectively discriminate between individuals (Figure 1, 4), their use raises important privacy concerns. Cross-dataset re-identification could inadvertently reveal sensitive information, such as clinical diagnoses or genetic risk factors. This risk should

be considered in further developments and uses of fingerprinting and related neurophysiological identification methods.

4.8 Conclusions

Overall, we've shown that MEG spectral fingerprints are highly robust maps for individual re-identification (Figure 1) but are minimally disrupted by early-stage Alzheimer's pathology (Tables 1, 2, 3). For AD patients, as the time to diagnosis increases, fingerprint distinctiveness tends to decline slightly (Figures 7a, 7b, 7d), but the effect is modest and its underlying cause remains unclear. So, while MEG fingerprints are not sole predictors of Alzheimer pre-diagnosis, they may still offer valuable complementary information when combined with other biomarkers or cognitive assessments. Therefore, further methodological advancements, especially methods capable of detecting subtle spectral deviations from an individual's baseline (such as spectral deviation mapping) and more frequent longitudinal assessments, will be critical to determine whether MEG fingerprints can transition from stable identifiers to early indicators of neurodegeneration.

References

[1] Finn, Emily S., Xilin Shen, Dustin Scheinost, Monica D. Rosenberg, Jian Huang, Michael M. Chun, and R. Todd Constable. "Functional Connectome Fingerprinting: Identifying Individuals Using Patterns of Brain Connectivity." *Nature Neuroscience*, vol. 18, no. 11, 12 Oct. 2015, pp. 1664–1671.

[2] da Silva Castanheira, Jason, Alex I. Wiesman, Justine Y. Hansen, Bratislav Misic, Sylvain Baillet, et al. "The Neurophysiological Brain-Fingerprint of Parkinson's Disease." *EBioMedicine*, vol. 105, July 2024, p. 105201. doi:10.1016/j.ebiom.2024.105201

[3] Gallego-Rudolf, Jonathan, Alex I. Wiesman, Alexa Pichet Binette, Sylvia Villeneuve, Sylvain Baillet, et al. "Synergistic Association of Ab and Tau Pathology with Cortical Neurophysiology and Cognitive Decline in Asymptomatic Older Adults." *Nature Neuroscience*, vol. 27, 18 Sept. 2024, pp. 2130–2137. doi:10.1038/s41593-024-01763-8

[4] Tadel, François, Sylvain Baillet, John C. Mosher, Dimitrios Pantazis, and Richard M. Leahy. "Brainstorm: A User-Friendly Application for MEG/EEG Analysis." *Computational Intelligence and Neuroscience*, vol. 2011, 2011, Article ID 879716, 13 pp. doi:10.1155/2011/879716

[5] Baillet, Sylvain. "Magnetoencephalography for Brain Electrophysiology and Imaging." *Nature Neuroscience*, vol. 20, no. 3, 23 Feb. 2017, pp. 327–339. doi:10.1038/nn.4504

[6] Desikan, Rahul S., Florent Ségonne, Bruce Fischl, Brian T. Quinn, Bradford C. Dickerson, Deborah Blacker, et al. "An Automated Labeling System for Subdividing the Human Cerebral Cortex on MRI Scans into Gyral Based Regions of Interest." *NeuroImage*, vol. 31, no. 3, 1 July 2006, pp. 968–980. doi:10.1016/j.neuroimage.2006.01.021

[7] Welch, Peter D. "The Use of Fast Fourier Transform for the Estimation of Power Spectra: A Method Based on Time Averaging Over Short, Modified Periodograms." *IEEE Transactions on Audio and Electroacoustics*, vol. AU-15, no. 2, June 1967, pp. 70–73. doi:10.1109/TAU.1967.1161901

[8] Amico, Enrico, and Joaquín Goñi. "The Quest for Identifiability in Human Functional Connectomes." *Scientific Reports*, vol. 8, no. 1, 6 May 2018, article 8254. doi:10.1038/s41598-018-25089-1